Electronic, magnetic and optical properties of half-Heusler alloy ZrCrPb: a DFT study

Student ID: 171332
Session: 2017-2018

Report submitted to the Department of Physics at
Jashore University of Science and Technology
in partial fulfillment of the requirements
for the degree of Bachelor of Science
with Honours in Physics

December 2022

Abstract

In this work, half-Heusler ZrCrPb alloy was studied utilizing the Full Potential Linear Augmented Plane Wave (FP-LAPW) method as implemented in the WIEN2k code in the context of Density Functional Theory (DFT). The goal of this research was to investigate the electronic, magnetic and optical properties of the half-Heusler alloy. For our study, we employ the Perdew-Burke-Ernzerhof (PBE) exchange-correlation potential for solving Kohn-Sham equation. The electronic band structures show that there is a band gap of 1.098 eV in up spin state and no band gap in down spin state of the computed alloy, which demonstrates the half metallic nature of the alloy ZrCrPb. The total magnetic moment is found to be around 4 μ_{B}, indicating that the alloy is ferromagnetic. The alloy's overall electrical and optical characteristics support its use in electromagnetic applications.

Acknowledgements

Firstly, I praise and thank Almighty Allah, the Lord of the worlds, the Most Merciful, the Guider of hearts, the Provider of sustenance, the Owner of life and death.

I would like to thank my respected supervisor, Dr. Mohammad Abdur Rashid, for his continuous supervision and constant guidance to complete my project work properly. During the period of this project, he always gave me invaluable confidence.

I am also grateful to the writers of several articles (included in the bibliography), from where I have gleaned a wealth of additional data. I would like to thank my group members and my classmates who helped me a lot.

I would never forget to pay thanks to my parents from the core of my heart for their love, unconditional supporting and prayers in all steps in my life. Their love and encouragement always give me mental support to continue my study smoothly.

Contents

List of Figures

List of Tables

Electronic, magnetic and optical properties of half-Heusler alloy ZrCrPb: a DFT study

Chapter 1

Introduction

In the last three decades, the search for new materials in the field of spintronics has led to Heusler alloys, which have proven to be excellent candidates for spin-based electronic devices. Spintronics is a branch of science concerned with the use of spin-directed materials in nano-scale devices such as spin-polarized light-emitting diodes [1–3], spin-polarized field-effect transistors [4–6], magnetic random access memories (MRAM) [7–9] and magnetic sensors etc [10, 11]. However, the production of these devices at ambient temperature is frequently challenging. This is because, at ambient temperature, the metals used to produce these devices lost their half metallicity resulting in relatively large magnetic moments. Furthermore, half-metallic materials with a large magnetic moment are not appropriate for practical spintronic applications. The most commonly employed materials in this sector are ferromagnets, ferrimagnets and anti-ferromagnets [12, 13]. Half metallic ferromagnets are a sort of novel materials with unique properties that are one of the most important components in spintronics [14]. Half-metallic (HM) materials, in which one of the two spin bands is semiconducting with a gap at the Fermi level but the other is metallic, resulting in 100% spin polarization at the Fermi level, are gaining in popularity due to their potential applications in spintronic devices. Heusler alloys show the properties required for spintronic application which was developed in 1903

by a German mining engineer and chemist Friedrich Heusler [15, 16], have been actively investigated in the scientific community both experimentally and theoretically for a long time. Heusler alloys can be synthesized with XYZ, X_2YZ, and XX′YZ chemical formulations as half-Heusler [17–20], full Heusler [21–23], and quaternary Heusler [24–28] alloys, respectively. Numerous investigations on these materials have already been undertaken, and many of them have gone on to become half-metallic ferromagnets. Interest in half-metal alloys has grown significantly since de Groot et al., discovered half-metallic features of NiMnSb and PtMnSb half-Heusler alloys [29]. The investigation of structural, electronic and magnetic properties of YCrSb and YMnSb was done by M. Atif Sattar [30]. The thermoelectric properties of LiZnSb and LiZnN were investigated by Manaj K. Yadav [31] and so many others. In the world of semiconductors, surface reconstruction has been a hot topic of study. It is also crucial for physics fundamental aspects. The findings of this research could be useful in determining the uses of half-Heusler alloys in the field of spintronics. In this article, we represent our theoretical investigation of electronic, magnetic, and optical properties of half-Heusler ZrCrPb alloy. The band structures, total and partial density of states, real and imaginary dielectric functions, absorptivity, conductivity, reflectivity and refractive index of calculated half-Heusler alloy are presented in this article.

Chapter 2

Background theory

2.1 Schrödinger equation

Schrödinger equation refers to a fundamental equation of quantum physics. The Schrödinger equation is a linear partial differential equation that governs the wave function of a quantum-mechanical system [32]. It is a key result in quantum mechanics, and its discovery was a significant landmark in the development of the subject. The equation is named after Erwin Schrödinger, who postulated the equation in 1925, and published it in 1926, forming the basis for the work that resulted in his Nobel Prize in physics in 1933 [33, 34]. The time-independent Schrödinger equation

$$\hat{H}\Psi(\vec{r}) = \hat{E}\Psi(\vec{r}) \tag{2.1}$$

Where, $\hat{H}$ is the hamiltonian operator and Ψ is the wave function. It is often impracticable to use a complete relativistic formulation of the formula; therefore Schrödinger himself postulated a non-relativistic approximation which is nowadays often used, especially in quantum chemistry. Using the Hamiltonian for a single particle

$$\hat{H} = \hat{T} + \hat{V} = -\frac{\hbar^2}{2m}\vec{\nabla}^2 + V(\vec{r}) \tag{2.2}$$

leads to the (non-relativistic) time-independent single-particle Schrödinger equation

$$\hat{E}\Psi(\vec{r}) = \Big[-\frac{\hbar^2}{2m}\vec{\nabla}^2 + V(\vec{r})\Big]\Psi(\vec{r}). \tag{2.3}$$

For N particles in three dimensions, the Hamiltonian is

$$\hat{H} = \sum_{i=1}^{N} \frac{\hat{p}_i^2}{2m_i} + V(\vec{r}_1, \vec{r}_2, ...\vec{r}_N) = -\frac{\hbar^2}{2}\sum_{i=1}^{N}\frac{1}{m_i} + V(\vec{r}_1, \vec{r}_2, ...\vec{r}_N) \tag{2.4}$$

The corresponding Schrödinger equation reads

$$\hat{E}\Psi(\vec{r}_1, \vec{r}_2, ...\vec{r}_N) = \Big[-\frac{\hbar^2}{2}\sum_{i=1}^{N}\frac{1}{m_i}\nabla_i^2 + V(\vec{r}_1, \vec{r}_2, ...\vec{r}_N)\Big]\Psi(\vec{r}_1, \vec{r}_2, ...\vec{r}_N) \tag{2.5}$$

Special cases are the solutions of the time-independent Schrödinger equation, where the Hamiltonian itself has no time-dependency (which implies a time-independent potential V $(\vec{r}_1, \vec{r}_2, ..., \vec{r}_N)$ and the solutions therefore describe standing waves which are called stationary states or orbitals). The time-independent Schrödinger equation is not only easier to treat, but the knowledge of its solutions also provides crucial insight to handle the corresponding time-dependent equation. The time-independent equation is obtained by the approach of separation of variables, i.e. the spatial part of the wave function is separated from the temporal part via [35]

$$\Psi(\vec{r}_1, \vec{r}_2, ..., \vec{r}_N, t) = \psi(\vec{r}_1, \vec{r}_2, ..., \vec{r}_N)\tau(t) = \psi(\vec{r}_1, \vec{r}_2, ..., \vec{r}_N)e^{\frac{iEt}{\hbar}} \tag{2.6}$$

Furthermore, the l.h.s. of the equation reduces to the energy eigenvalue of the Hamiltonian multiplied by the wave function, leading to the general eigenvalue equation

$$E\psi(\vec{r}_1, \vec{r}_2, ...\vec{r}_N) = \hat{H}\psi(\vec{r}_1, \vec{r}_2, ...\vec{r}_N) \tag{2.7}$$

Again, using the many-body Hamiltonian, the Schrödinger equation becomes

$$E\psi(\vec{r}_1, \vec{r}_2, ..., \vec{r}_N) = \Big[-\frac{\hbar^2}{2}\sum_{i=1}^{N}\frac{1}{m_i}\nabla_i^2 + V(\vec{r}_1, \vec{r}_2, ..., \vec{r}_N)\Big]\psi(\vec{r}_1, \vec{r}_2, ..., \vec{r}_N) \tag{2.8}$$

2.1.1 The wave function

Wave function ψ is a quantity associated with a moving particle. It is a complex quantity. The wave function ψ has no direct physical meaning. The wave function $\psi(r,t)$ describes the position of a particle with respect to time. It can be considered as probability amplitude. $|\psi|^2$ is proportional to the probability of finding a particle at a particular time. It is the probability density.

$$|\psi|^2 = |\psi^*\psi|^2 \tag{2.9}$$

The wave function ψ must be finite everywhere. If ψ is finite for a particular point, it means an infinite large probability of finding the particles at that point. This would violates the uncertainty principle. It must be single valued. If ψ has more than one value at any point, it means more than one value of probability of finding the particle at that point which is obviously ridiculous. The wave function must be continuous and have a continuous first derivative everywhere and its must be normalizable. For the sake of simplicity the discussion is restricted to the time-independent wave function. A question always arising with physical quantities is about possible interpretations as well as observations. The Born probability interpretation of the wave function, which is a major principle of the Copenhagen interpretation of quantum mechanics, provides a physical interpretation for the square of the wave function as a probability density [36, 37]

$$P = |\psi(\vec{r}_1, \vec{r}_2, ..., \vec{r}_N|^2 d\vec{r}_1 d\vec{r}_2 .... d\vec{r}_N \tag{2.10}$$

Equation (2.10) describes the probability that particles 1,2,...,N are located simultaneously in the corresponding volume element $d\vec{r}_1\ d\vec{r}_2 ... d\vec{r}_N$ [38]. What happens if the positions of two particles are exchanged, must be considered as well. Following merely logical reasoning, the overall probability density cannot depend on such an exchange, i.e.

$$|\psi(\vec{r}_1, \vec{r}_2, ..., \vec{r}_i, \vec{r}_j, ..., \vec{r}_N)|^2 = |\psi(\vec{r}_1, \vec{r}_2, ..., \vec{r}_j, \vec{r}_i, ..., \vec{r}_N)|^2 \tag{2.11}$$

There are only two possibilities for the behavior of the wave function during a particle exchange. The first one is a symmetrical wave function, which does not change due to such an exchange. This corresponds to bosons (particles with integer or zero spin). The other possibility is an anti-symmetrical wave function, where an exchange of two particles causes a sign change, which corresponds to fermions (particles which half-integer spin) [39, 40]. In this text only electrons are from interest, which are fermions. The anti symmetric fermion wave function leads to the Pauli principle, which states that no two electrons can occupy the same state, whereas state means the orbital and spin parts of the wave function [41] (the term spin coordinates will be discussed later in more detail). The antisymmetry principle can be seen as the quantum-mechanical formalization of Pauli's theoretical ideas in the description of spectra (e.g. alkaline doublets) [42]. Another consequence of the probability interpretation is the normalization of the wave function. If equation (2.10) describes the probability of finding a particle in a volume element, setting the full range of coordinates as volume element must result in a probability of one, i.e. all particles must be found somewhere in space. This corresponds to the normalization condition for the wave function.

$$\int d\vec{r}_1 \int d\vec{r}_2 ... \int d\vec{r}_N |\psi(\vec{r}_1, \vec{r}_2, ..., \vec{r}_N)|^2 = 1 \tag{2.12}$$

Equation (2.12) also gives insight on the requirements a wave function must fulfill in order to be physical acceptable. Wave functions must be continuous over the full spatial range and square-integratable [43]. Calculating the expectation values of operators with a wave function also provides the expectation value of the relevant observable for that wave function [44]. For an observable $\mathrm{O}(\vec{r}_1, \vec{r}_2, ..., \vec{r}_N)$, this can generally be written as

$$O = \langle O \rangle = \int d\vec{r}_1 \int d\vec{r}_2 ... \int d\vec{r}_N \psi^*(\vec{r}_1, \vec{r}, ..., \vec{r}_N) \hat{O} \psi(\vec{r}_1, \vec{r}_2, ..., \vec{r}_N) \tag{2.13}$$

2.2 Born-Oppenheimer (BO) approximation

The Hamiltonian of a many-body system consisting of nuclei and electrons can be written as:

$$H_{tot} = -\sum_{I} \frac{\hbar^2}{2M_I}\nabla^2_{\vec{R}_I} - \sum_{i} \frac{\hbar^2}{2m_e}\nabla^2_{\vec{r}_i} + \frac{1}{2}\sum_{\substack{I,J \\ I\neq J}} \frac{Z_I Z_J e^2}{|\vec{R}_I - \vec{R}_J|} + \frac{1}{2}\sum_{\substack{i,j \\ i\neq j}} \frac{e^2}{|\vec{r}_i - \vec{r}_j|} - \sum_{I,i} \frac{Z_I e^2}{|\vec{R}_I - \vec{r}_i|} \tag{2.14}$$

Where the indexes I, J run on nuclei, i and j on electrons, $\vec{R}_I$ and M_I are positions and masses of the nuclei, $\vec{r}_i$ and m_e of the electrons, Z_I the atomic number of nucleus I. The first term is the kinetic energy of the nuclei, the second term is the kinetic energy of the electrons, the third term is the potential energy of nucleus-nucleus Coulomb interaction, the fourth term is the potential energy of electron-electron Coulomb interaction and the last term is the potential energy of nucleus-electron Coulomb interaction. The time-independent Schrödinger equation for the system is,

$$H_{tot}\Psi(\{\vec{R}_I\},\{\vec{r}_i\}) = E\Psi(\{\vec{R}_I\},\{\vec{r}_i\}) \tag{2.15}$$

Where $\Psi(\{\vec{R}_I\},\{\vec{r}_i\})$ is the total wave function of the system. By solving the above Schrödinger equation we get wave function, which can provide everything about the system. It is quietly impossible to solve it in practice and approximation is needed. A so-called Born-Oppenheimer approximation was made by Born and Oppenheimer in 1927. Since the nuclei are much heavier than electrons, the nuclei move much slower than the electrons. Therefore we can separate the movement of nuclei and electrons. So, the electronic wave function depends upon only the nuclear position but does not depend upon their velocities. The total wave function can be written as

$$\Psi(\{\vec{R}_I\},\{\vec{r}_i\}) = \Theta(\{\vec{R}_I\})\phi(\{\vec{r}_i\};\{\vec{R}_I\}) \tag{2.16}$$

Where $\Theta(\{\vec{R}_I\})$ describe the nuclei and $\phi(\{\vec{r}_i\};\{\vec{R}_I\})$ the electrons. So, we can write the Schrödinger equation into two separate equation.

$$H_e\phi(\{\vec{r}_i\};\{\vec{R}_I\}) = V(\{\vec{R}_I\})\phi(\{\vec{r}_i\};\{\vec{R}_I\}) \tag{2.17}$$

Where,

$$H_e = -\sum_i \frac{\hbar^2}{2m_e}\nabla^2_{\vec{r}_i} + \frac{1}{2}\sum_{\substack{I,J \\ I\neq J}} \frac{Z_I Z_J e^2}{|\vec{R}_I - \vec{R}_J|} + \frac{1}{2}\sum_{\substack{i,j \\ i\neq j}} \frac{e^2}{|\vec{r}_i - \vec{r}_j|} - \sum_{I,i} \frac{Z_I e^2}{|\vec{R}_I - \vec{r}_i|} \tag{2.18}$$

and

$$\left[-\sum_I \frac{\hbar^2}{2M_I}\nabla^2_{\vec{R}_I} + V(\{\vec{R}_I\}) \right] \Theta(\{\vec{R}_I\}) = E'\Theta(\{\vec{R}_i\}) \tag{2.19}$$

Equation (2.17) is the equation for the electronic problem with the nuclei positions fixed. The significance of the BO approximation is to separate the movement of electrons and nuclei.

2.3 The Hartree-Fock approach

In order to find a suitable strategy to approximate the analytically not accessible solutions of many-body problems, a very useful tool is variational calculus, similar to the least-action principle of classical mechanics. By the use of variational calculus, the ground state wave function ψ_0, which corresponds to the lowest energy of the system E_0, can be approached. A useful literature source for the principles of variational calculus has been provided by T. Flieÿbach [45]. Hence, for now only the electronic Schrödinger equation is of interest, therefore in the following sections we set $\hat{H} \equiv \hat{H}_e l$, $E \equiv E_e l$, and so on. Observables in quantum mechanics are calculated as the expectation values of operator. The energy as observable corresponds to the Hamilton operator, therefore the energy corresponding to a general Hamiltonian can be calculated as

$$E = \langle \hat{H} \rangle = \int d\vec{r}_1 \int d\vec{r}_2 ... \int d\vec{r}_N \psi * (\vec{r}_1, \vec{r}_2, ..., \vec{r}_N) \hat{H} \psi(\vec{r}_1, \vec{r}_2, ..., \vec{r}_N) \tag{2.20}$$

The Hatree-Fock techique is based on the principle that the energy obtained by any (normalized) trial wave function other than the actual ground state wave function is always an upper bound, i.e. higher than the actual ground state energy. If the trial function happens to be the desired ground state wave function, the energies

are equal to

$$E_{trial} \geq E_0 \tag{2.21}$$

with

$$E_{trial} = \int d\vec{r}_1 \int d\vec{r}_2 ... \int d\vec{r}_N \psi^*_{trial}(\vec{r}_1, \vec{r}_2, ..., \vec{r}_N) \hat{H} \psi_{trial}(\vec{r}_1, \vec{r}_2, ..., \vec{r}_N) \tag{2.22}$$

and

$$E_0 = \int d\vec{r}_1 \int d\vec{r}_2 ... \int d\vec{r}_N \psi^*_0(\vec{r}_1, \vec{r}_2, ..., \vec{r}_N) \hat{H} \psi_0(\vec{r}_1, \vec{r}_2, ..., \vec{r}_N) \tag{2.23}$$

The expressions above are usually inconvenient to handle. For the sake of a compact notation, in the following the bra-ket notation of Dirac is introduced. For a detailed description of this notation, the reader is referred to the original publication [46]. In that notation, equation (2.21) to (2.23) are expressed as

$$\langle \psi_{trial} | \hat{H} | \psi_{trial} \rangle = E_{trial} \geq E_0 = \langle \psi_0 | \hat{H} | \psi_0 \rangle \tag{2.24}$$

Proof: The eigenfunctions ψ_i of the Hamiltonian $\hat{H}$ (each corresponding to an energy eigenvalue E_i form a complete basis set, therefore any normalized trial wave function ψ_{trial} can be expressed as linear combination of those eigenfunctions.

$$\psi_{trial} = \sum_i \lambda_i \psi_i \tag{2.25}$$

The assumption is made that the eigenfunctions are orthogonal and normalized. Hence it is requested that the trial wave function is normalized, it follows that

$$\langle \psi_{trial} | \psi_{trial} \rangle = 1 = \langle \sum_i \lambda_i \psi_i | \sum_j \lambda_j \psi_j \rangle = \sum_i \sum_j \lambda_i^* \lambda_j \langle \psi_i | \psi_j \rangle = \sum_j |\lambda_j|^2 \tag{2.26}$$

On the other hand, following (2.24) and (2.26)

$$E_{trial} = \langle \psi_{trial} | \hat{H} | \psi_{trial} \rangle = \langle \sum_i \lambda_i \psi_i | \hat{H} | \sum_j \lambda_j \psi_j \rangle = \sum_j E_j |\lambda_j|^2 \tag{2.27}$$

Together with the fact that the ground state energy E_0 is per definition the lowest possible energy, and therefore has the smallest eigenvalue ($E_0 \leq E_i$), it is found that

$$E_{trial} = \sum_j E_j |\lambda_j|^2 \geq E_0 \sum_j |\lambda_j|^2 \tag{2.28}$$

what resembles equation (2.24). The mathematical framework used above, i.e. rules which assign numerical values to functions, so called functionals, is also one of the main concepts in density functional theory. A function gets a numerical input and generates a numerical output whereas a functional gets a function as input and generates a numerical output [47]. Equations (2.20) to (2.28) also include that a search for the minimal energy value while applied on all allowed N electron wave-functions will always provide the ground-state wave function (or wave functions, in case of a degenerate ground state where more than one wave function provides the minimum energy). Expressed in terms of functional calculus,where $\psi \to N$ addresses all allowed N-electron wave functions, this means

$$E_0 = \min_{\psi \to N} E[\psi] = \min_{\psi \to N} \langle \psi | \hat{H} | \psi \rangle = \min_{\psi \to N} \langle \psi | \hat{T} + \hat{V} + \hat{U} | \psi \rangle \tag{2.29}$$

Due to the vast number of alternative wave functions on the one hand and processing power and time constraints on the other, this search is essentially unfeasible for N electron systems. Restriction of the search to a smaller subset of potential wave functions, as in the Hartree-Fock approximation, is conceivable. A slater determinant is a formula in quantum mechanics that desceibes the wave function of a multi-fermionic system. It satisfies anti-symmetric criteria, and thus the Pauli's principle, by changing sign when two electrons are exchanged (or other fermions). Only a small fraction of all potential fermionic wave functions can be expressed as a single slater determinant, but because of their simplicity, they are an important and useful subset. In the Hartree- Fock approach, the search is restricted to approximations of the N-electron wave function by an antisymmetric product of N (normalized) one electron wave functons, the so called spin- orbitals $\chi_i(\vec{x}_i)$. A wave

function of this type is called Slater-determinant, and reads

$$\Psi_0 \approx \phi_{SD} = (N!)^{-\frac{1}{2}} \begin{vmatrix} \chi_1(\vec{x}_1) & \chi_2(\vec{x}_1) & \cdots & \chi_N(\vec{x}_1) \\ \chi_1(\vec{x}_2) & \chi_2(\vec{x}_2) & \cdots & \chi_N(\vec{x}_2) \\ \vdots & \vdots & \ddots & \vdots \\ \chi_1(\vec{x}_N) & \chi_2(\vec{x}_N) & \cdots & \chi_N(\vec{x}_N) \end{vmatrix} \tag{2.30}$$

It is important to notice that the spin-orbitals $\chi_i(\vec{x}_i)$ are not only depending on spatial coordinates but also on a spin coordinate which is introduced by a spin function, $\vec{x}_i = \vec{r}_i, s$. Returning to the variational principle and equation (2.29), the ground state energy approximated by a single slater determinant becomes

$$E_0 = \min_{\phi_{SD} \to N} E[\phi_{SD}] = \min_{\phi_{SD} \to N} \langle \phi_{SD} | \hat{H} | \phi_{SD} \rangle = \min_{\phi_{SD} \to N} \langle \phi_{SD} | \hat{T} + \hat{V} + \hat{U} | \phi_{SD} \rangle \tag{2.31}$$

A general expression for the Hartree-Fock Energy is obtained by usage of the Slater determinant as a trial function

$$E_{HF} = \langle \phi_{SD} | \hat{H} | \phi_{SD} \rangle = \langle \phi_{SD} | \hat{T} + \hat{V} + \hat{U} | \phi_{SD} \rangle \tag{2.32}$$

For the sake of brevity, a detailed derivation of the final expression for the Hartree-Fock energy is omitted. It is a straightforward calculation found for example in the Book by Schwabl. The final expression for the Hartree-Fock energy contains three major parts:

$$E_{HF} = \langle \phi_{SD} | \hat{H} | \phi_{SD} \rangle = \sum_i^N (i|\hat{h}|i) + \frac{1}{2} \sum_i^N \sum_j^N [(ii|jj) - (ij|ji)] \tag{2.33}$$

with

$$(i|\hat{h_i}|i) = \int \chi_i^*(\vec{x}_i)[-\frac{1}{2}\vec{\nabla}_i^2 - \sum_{k=1}^M \frac{Z_k}{r_{ik}}]\chi_i(\vec{x}_i) d\vec{x}_i, \tag{2.34}$$

$$(ii|jj) = \iint |\chi_i(\vec{x}_i)|^2 \frac{1}{r_{ij}} |\chi_j(\vec{x}_j)|^2 d\vec{x}_i d\vec{x}_j, \tag{2.35}$$

$$(ii|jj) = \iint \chi_i(\vec{x}_i)\chi_j^*(\vec{x}_j) \frac{1}{r_{ij}} \chi_j(\vec{x}_j)\chi_i^*(\vec{x}_i) d\vec{x}_i d\vec{x}_j \tag{2.36}$$

The first term corresponds to the kinetic energy and the nucleus-electron interactions, $\hat{h}$ denoting the single particle contribution of the Hamiltonian, whereas the latter two terms correspond to electron-electron interactions. They are called Coulomb and exchange integral, respectively. Examination of equations (2.33) to (2.36) furthermore reveals, that the Hartree-Fock energy can be expressed as a functional of the spin orbitals $E_{HF} = E[\{\chi_i\}]$. Thus, variation of the spin orbitals leads to the minimum energy. An important point is that the spin orbitals remain orthonormal during minimization.This restriction is accomplished by the introduction of Lagrangian multipliers λ_i in the resulting equations, which represent the Hartree-Fock equations. Finally one arrives at

$$\hat{f}\chi_i = \lambda_i \chi_i \qquad i = 1, 2, ..., N \tag{2.37}$$

with

$$\hat{f}_i = -\frac{1}{2}\vec{\nabla}_i^2 - \sum_{k=1}^{M} \frac{Z_k}{r_{ik}} + \sum_{i}^{N} [\hat{J}_j(\vec{x}_i) - \hat{K}_j(\vec{x}_i)] = \hat{h}_i + \hat{V}^{HF}(i) \tag{2.38}$$

the Fock operator for the i-th electron. In similarity to (2.33) to (2.36), the first twonterms represent the kinetic and potential energy due to nucleus-electron interaction, collected in the core Hamiltonian $\hat{h}_i$, whereas the latter terms are sums over the Coulomb operators $\hat{J}_j$ and the exchange operators $\hat{K}_j$ with the other j electrons, which form the Hartree-Fock potential $\hat{V}^{HF}$. There are major approximation of Hartree-Fock can be seen. The two electron repulsion operator from the original Hamiltonian is exchanged by a one-electron operator $\hat{V}^{HF}$ which describes the repulsion in average.

2.3.1 Limitations and failings of the Hartree-Fock approach

Atoms as well as molecules can have an even or odd number of electrons. If the number of electrons is even and all of them are located in double occupied spatial orbitals ϕ_i, the compound is in a singlet state. Such systems are called closed-shell systems. Compounds with an odd number of electrons as well as compounds with single occupied orbitals, i.e. species with triplet or higher ground state, are called open-shell systems respectively. These two types of systems correspond to two dif-

ferent approaches of the Hartree-Fock method. In the restricted HF method (RHF), all electrons are considered to be paired in orbitals whereas in the unrestricted HF method (UHF) this limitation is lifted totally. It is also possible to describe open-shell systems with a RHF approach where only the single occupied orbitals are excluded which is then called a restricted open-shell HF (ROHF) which is an approach closer to reality but also more complex and therefore less popular than UHF. There are also closed-shell systems which require the unrestricted approach in order to get proper results. For instance, the description of the dissociation of H_2 (i.e.) the behavior at large internuclear distance), where one electron must be located at one hydrogen atom, can logically not be obtained by the use of a system which places both electrons in the same spatial orbital. Therefore the choice of method is always a very important point in HF calculations. Kohn states several $M = p^5$ with $3 \leq p \leq 10$ parameters for an output with adequate accuracy in the investigations of the H_2 system [48]. For a system with $N = 100$ electrons, the number of parameters rises to

$$M = p^{3N} = 3^{300} to 10^{300} \approx 10^{150} to 10^{300} \tag{2.39}$$

According to the equation (2.39), energy reduction would have to be done in a space with at least 10^{150} dimension, which is well above current computer capabilities. As a result, HF methods are limited to situations involving a modest number of electron ($N \approx 10$), This barrier commonly referred to as the exponential wall because of the exponential component in (2.39) [48]. Since a many electron wave function cannot be described entirely by a single Slater determinant, the energy obtained by HF calculations is always larger than the exact ground state energy. The most accurate energy obtainable by HF methods is called the Hartree-Fock-limit. The difference between E_{HF} and E_{exact} is called correlation energy and can be denoted as [49]

$$E_{corr}^{HF} = E_{min} - E_{HF} \tag{2.40}$$

2.4 The electron density

A general statement concerning the computation of observablees has been presented in section 2.1.1 about the wave function ψ. This section is about a quantity that is computed in a similar manner. The electron density (for N electrons) as the basic variable of density functional theory is defined as [38]

$$n(\vec{x}) = N \sum_{s_1} \int d\vec{x}_2 ... \int d\vec{x}_N \psi^*(\vec{x}_1, \vec{x}_2, ..., \vec{x}_N)\psi(\vec{x}_1, \vec{x}_2, ..., \vec{x}_N). \tag{2.41}$$

which is the basic variable of density function theory. If the spin coordinates are neglected, the electron density can even be expressed as measurable observable only dependent on spatial coordinates

$$n(\vec{r}) = N \int d\vec{r}_2 ... \int d\vec{r}_N \psi^*(\vec{r}_1, \vec{r}_2, ..., \vec{r}_N)\psi(\vec{r}_1, \vec{r}_2, ..., \vec{r}_N) \tag{2.42}$$

The total number of electrons can be obtained by integration the electron density over the spatial variables

$$N = \int d\vec{r} n(\vec{r}). \tag{2.43}$$

2.5 Thomas-Fermi Model

The predecessor to DFT was the Thomas-Fermi (TF) model proposed by Thomas amd Fermi in 1927. In this method, they used the electron density $n(\mathbf{r})$ as the basic variable instead of the wave function. The total energy of a system in an external potential $V_{ext}(\mathbf{r})$ is written as a function of the electron density $n(\mathbf{r})$ as:

$$E_{TF}[n(\mathbf{r})] = A_1 \int n(\mathbf{r})^{\frac{5}{3}} d\mathbf{r} + \int n(\mathbf{r}) V_{ext}(\mathbf{r}) d\mathbf{r} + \frac{1}{2} \iint \frac{n(\mathbf{r})n(\mathbf{r}')}{|\mathbf{r} - \mathbf{r}'|} d\mathbf{r} d\mathbf{r}' \tag{2.44}$$

where the first term is the kinetic energy of the non-interacting electron in a homogeneous electron gas (HEG) with $A_1 = \frac{3}{10}(3\pi^2)^{\frac{2}{3}}$ in the atomic units. The free

electron energy state $\varepsilon_k = \frac{k^2}{2}$ up to the fermi wave vector $k_F = [3\pi^2 n(\mathbf{r})]^{\frac{1}{3}}$ as:

$$t_0[n(\mathbf{r})] = \frac{2}{(2\pi)^3}\int_0^{k_F}\frac{k^2}{2}4\pi k^2 dk = A_1 n(\mathbf{r})^{\frac{5}{3}} \tag{2.45}$$

In 1930, Dirac extended the Thomas-Fermi method by adding a local exchange term $A_2\int n(\mathbf{r})^{\frac{3}{4}}d\mathbf{r}$ to Equation (2.44) with $A_2 = -\frac{3}{4}(\frac{3}{\pi})^{\frac{1}{3}}$ which leads Equation (2.44) to

$$E_{TFD}[n(\mathbf{r})] = A_1\int n(\mathbf{r})^{\frac{5}{3}}d\mathbf{r} + \int n(\mathbf{r})V_{ext}(\mathbf{r})d\mathbf{r} + \frac{1}{2}\iint\frac{n(\mathbf{r})n(\mathbf{r}')}{|\mathbf{r}-\mathbf{r}'|}d\mathbf{r}d\mathbf{r}' + A_2\int n(\mathbf{r})^{\frac{4}{3}}d\mathbf{r} \tag{2.46}$$

By using the technique of Lagrange multipliers, the solution can be found in the stationary condition:

$$\delta\{E_{TED}[n(\mathbf{r})] - \mu(\int n(\mathbf{r})d\mathbf{r} - N)\} = 0 \tag{2.47}$$

where μ is a constant known as a Lagrange multiplier, whose physical meaning is the chemical potential. Equation (2.47) leads to the Thomas-Fermi-Dirac equation,

$$\frac{5}{3}A_1 n(\mathbf{r})^{\frac{2}{3}} + V_{ext}(\mathbf{r}) + \int\frac{n(\mathbf{r}')}{|\mathbf{r}-\mathbf{r}'|}d\mathbf{r}' + \frac{4}{3}A_2 n(\mathbf{r})^{\frac{1}{3}} - \mu = 0 \tag{2.48}$$

This can be solved directly to obtain the ground state density.

2.6 The Hohenberg-Kohn (HK) theorems

DFT was proven to be an exact theory of many-body systems by Hohenberg and Kohn [51] in 1964. It applies not only to condensed-matter systems of electrons with fixed nuclei, but also more to any system of interacting particles in an external potential $V_{ext}(\vec{r})$. The theory is based upon two theorems.

2.6.1 HK theorem I

Statement: The ground state particle density $n(\mathbf{r})$ of a system of interacting particles in an external potential $V_{ext}(\mathbf{r})$ uniquely determines the external potential $V_{ext}(\mathbf{r})$, except for a constant. Thus the ground state particle density determines

the full Hamiltonian, except for a constant shift of the energy. In principle, all the states including ground and excited states of the many-body wavefunctions can be calculated. This means that the ground state particle density uniquely determines all properties of the system completely.

Proof: Here we only consider the case that the ground state of the system is nondegenerate. It can be proven that the theorem is also valid for systems with degenerate ground state [52]. Suppose there are two different external potentials $V_{ext}(\mathbf{r})$ and $V'_{ext}(\mathbf{r})$ whice differ by more than a constant and lead to the same ground state density $n_0(\mathbf{r})$. The two external potentials would give two different Hamiltonians, Ψ and Ψ', with $\hat{H}\Psi = E_0\Psi$ and $\hat{H}'\Psi' = E'_0\Psi'$. Since Ψ' is not the ground state of $\hat{H}$, it follows that

$$\begin{aligned} E_0 &< \langle\Psi'|\hat{H}|\Psi'\rangle \\ &< \langle\Psi'|\hat{H}'|\Psi'\rangle + \langle\Psi'|\hat{H} - \hat{H}'|\Psi'\rangle \\ &< E'_0 + \int n_0(\mathbf{r})\Big[V_{ext}(\mathbf{r}) - V'_{ext}(\mathbf{r})\Big]d\mathbf{r} \end{aligned} \tag{2.49}$$

Similarly

$$\begin{aligned} {E_0}' &< \langle\Psi|\hat{H}'|\Psi\rangle \\ &< \langle\Psi|\hat{H}|\Psi\rangle + \langle\Psi|\hat{H}' - \hat{H}|\Psi\rangle \\ &< E_0 + \int n_0(\mathbf{r})\Big[V'_{ext}(\mathbf{r}) - V_{ext}(\mathbf{r})\Big]d\mathbf{r} \end{aligned} \tag{2.50}$$

Adding Equations (2.49) and (2.50) lead to the contradiction

$$E_0 + E'_0 < E_0 + E'_0 \tag{2.51}$$

Hence, no two different external potentials $V_{ext}(\mathbf{r})$ can give rise to the same ground state density $n_0(\mathbf{r})$,i.e., the ground state density determines the external potential $V_{ext}(\mathbf{r})$, except for a constant.That is to say, there is a one-to-one mapping between

the ground state density $n_0(\mathbf{r})$ and the external potential $V_{ext}(\mathbf{r})$, although the exact formula is known.

2.6.2 HK theorem II

Statement: The ground state energy can be derived from the electron density by the use of variational calculus. The electron density, which provides a minimum of the ground state energy, is therefore the exact ground state density. Since the wave function is a unique functional of the electron density, every trial wave function Ψ' corresponds to a trial density $n'(\vec{r})$ following equation(2.41). According to the Rayleigh-Ritz principle, the ground state energy is obtained as

$$E_{v,0} = \min_{\Psi'} \langle \Psi' | \hat{H} | \Psi' \rangle \tag{2.52}$$

Proof: In principle, the minimization can be carried out in two steps. In the first step, a trial electron density $n'(\vec{r})$ is fixed. The class of trial functions corresponding to that electron density is then denoted by $\Psi'^{\alpha}_{n'}$. Then, the constrained energy minimum is defined as

$$[E_v[n'(\vec{r})]] \equiv \min_{\alpha} \langle \Psi'^{\alpha}_{n'} | \hat{H} | \Psi'^{\alpha}_{n'} \rangle = \int v(\vec{r}) n'(\vec{r}) d\vec{r} + F[n'(\vec{r})]. \tag{2.53}$$

In that notation, $F[n'(\vec{r})]$ is the universal functional

$$F[n'(\vec{r})] \equiv \min_{\alpha} \langle \Psi'^{\alpha}_{n'} | \hat{T} + \hat{U} | \Psi'^{\alpha}_{n'} \rangle \tag{2.54}$$

Equation (2.55) is minimized over all trial densities $n'(\vec{r})$:

$$E_{v,0} = \min_{n'(\vec{r})} E_v[n'(\vec{r})] = \min_{n'(\vec{r})} \{ \int v(\vec{r}) n'(\vec{r}) d\vec{r} + F[n'(\vec{r})] \} \tag{2.55}$$

Now, for a non-degenerate ground state, the energy in 2.57 is attained, if $n'(\vec{r})$ is the actual ground state density. It has been shown that density functional theory provides a clear and mathematical exact framework for the use of the electron density as base variable. Nevertheless, nothing of what has been derived is of practical use.

In other words, the Hohenberg-Kohn theorems, as important as they are, do not provide any help for the calculation of molecular properties and also do not provide any information about approximations for functional like $F[n'(\vec{r})]$. This difficulties was overcome by Kohn and Sham in 1965, who proposed the well known Kohn-Sham equations.

2.7 Kohn-Sham equations

Kohn and Sham introduced an orbital approach for evaluating $F_{ni}[n]$ in 1965, which was an important step toward quantitative modeling of electronic structure. In other words, in order to evaluate the kinetic energy of N non interacting particles given only their density distribution $n(\mathbf{r})$, they simply found the corresponding potential, called $v_{eff}(\mathbf{r})$, and used the Schrödinger equation.

$$(-\frac{\hbar^2}{2M}\nabla^2 + v_{eff}(\mathbf{r}))\psi_i(\mathbf{r}) = \epsilon_i\psi_i(\mathbf{r}) \tag{2.56}$$

Such that $n(\mathbf{r}) = \sum_{i=1}^{N} |\psi(\mathbf{r})|^2$ the states ψ_i here are ordered so that the energies ϵ_i are non decreasing, and the spin index is included in i. If the ϵ_N is degenerate with ϵ_{N+1} (and also at finite temperatures), fractional occupations f_i are to be used $n(\mathbf{r}) = \sum_{i=1}^{\infty} f_i|\psi(\mathbf{r})|^2$, but if only spin degeneracy is involved, the result for the density is not affected. The kinetic energy is then given by,$F_{ni} = \sum_{i=1}^{N} |\langle\psi_i|\hat{t}|\psi_i\rangle = \sum_{i=1}^{N} \epsilon_i - \int d(\mathbf{r})n(\mathbf{r})v_{eff}(\mathbf{r})$ where $\hat{t}_i$ is the kinetic energy operator for the ith electron ($\hat{T} = \sum_i \hat{t}_i$). In practice, it is the external potential of a given system which is known, not the density distribution or the effective potential. One may find the effective potential by taking a functional derrivative of the three term expression for $F_{HK}[n]$, and rearranging the terms:

$$v_{eff}(\mathbf{r}) = v(\mathbf{r}) - e\varphi(\mathbf{r}) + XC(\mathbf{r}) \tag{2.57}$$

where we have used Equation (2.55) for both the interacting and non interacting system. The electrostatic potential is here

$$\varphi(\mathbf{r}) = -e \int d\mathbf{r}' \frac{n(\mathbf{r}')}{|\mathbf{r} - (\mathbf{r}')|} \tag{2.58}$$

And the exchange-correlation potential is defined as

$$v_{XC}(\mathbf{r}) = \frac{\delta E_{XC}}{\delta n(\mathbf{r})} \tag{2.59}$$

Given a particular approximation for $E_{XC}(n)$, one obtains $v_{XC}(\mathbf{r})$ and can thus find $v_{eff}(\mathbf{r})$ from $n(\mathbf{r})$ for a given $v(\mathbf{r})$. The set of equations described above is called the Kohn Sham equations of DFT [53–56].

2.7.1 Solving Kohn-Sham equations

Once we have approximated the exchange-correlation energy, we are in a position to solve the Kohn-Sham equations. The Kohn-Sham equations have an iterative solution; they have to be solved self-consistently. To solve the Kohn-Sham equations for a many body system, we need to define the Hartree potential and the exchange-correlation potential, and to define the Hartree potential and the exchange-correlation potential, we need to know the electron density $n(\mathbf{r})$. However, to find the electron density, we must know the single electron wave functions. We do not know these wave functions until we solve the Kohn-Sham equations. The well-known approach to solve the Kohn-Sham equations is to start with an initial trial electron density as illustrated in Figure 2.1. Then solve these equations using trial electron density. After solving the Kohn-Sham equations, we will have a set of single electron wave functions. Using these wave functions, we can calculate the new electron density. The new electron density in an input for the next cycle. Finally, compare the difference between the calculated electron densities for consecutive iterations. If the difference in electron density between consecutive iteration is lower than an appropriately chosen convergence criterion, then the solution of the Kohn-Sham equations is said to be self-consistent. Now the calculated electron density is considered as the ground state electron density, and it can be used to calculate the total energy of the

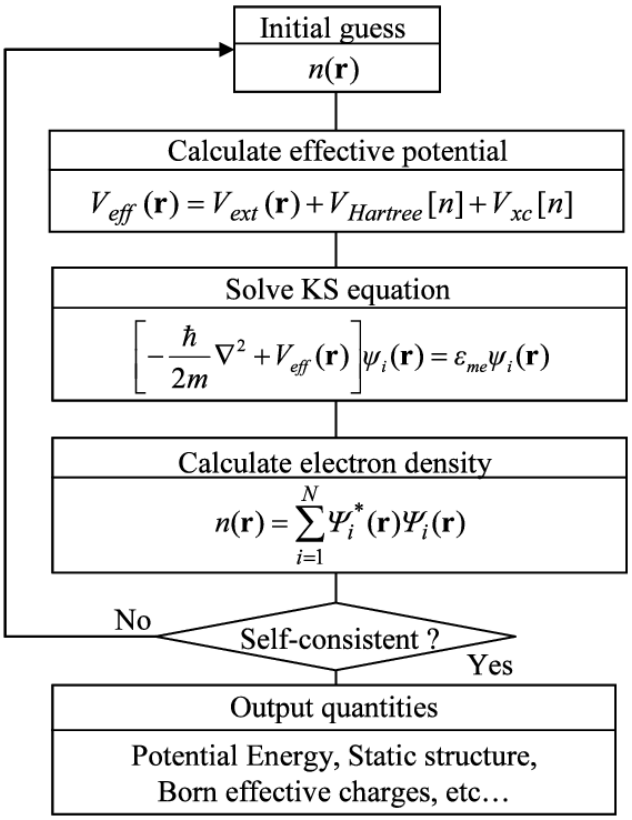

Figure 2.1: Flowchart of self-consistency loop for solving Kohn-Sham equations system.

2.8 The Exchange-Correlation Functional

The major problem in solving the Kohn-Sham equations is that the true form of the exchange-correlation functional is not known. Two main approximation methods have been implemented to approximate the exchange-correlation functional. The local density approximation (LDA) is first approach to approximate the exchange-correlation functional in DFT calculations. The second well known class of approximations to the Kohn-Sham exchange-correlation functional is the generalized gradient approximation (GGA). In the GGA approximation the exchange and correlations energies include the local electron density and the local gradient in the electron density [57].

Chapter 3

Electronic, magnetic and optical properties of ZrCrPb

3.1 Computational details

The full potential linear augmented plane wave (FP-LAPW) method [58], as implemented in WIEN2k [59] code, was used to calculate the half-Heusler ZrCrPb alloy inside density functional theory (DFT) [60]. In the Kohn-Sham (KS) equation [61], we use the Perdew-Burke-Ernzerhof (PBE) [62] functional to determine exchange-correlation (XC) potential. We use spin-polarized density functional theory in our calculations to account for the role of spin in the geometry optimization of electronic structure and magnetic behaviour. The energy convergence criteria was set to 10^{-5} R_y, while the charge convergence criteria was set to 10^{-4} e, where, e is an electron charge. The value of $R_{MT}K_{max}$ was set to 8 for alloy to limit the number of plane waves, where R_{MT} is the Muffin-Tin Radius and K_{max} is the maximum value selected for the expansion of the complete plane wave vector. R_{MT} values of Pb, Zr and Cr were 2.5, 2.5 and 2.48 respectively. The usual tetrahedron technique [63] was used to complete the Brillouin zone (BZ) integration.

3.2 Structural optimization

In Wyckoff coordinates, the Heusler structure can be thought of as four inter-penetrating face centered cubic (fcc) lattices with four unique crystal-sites. General formula for a half-Heusler alloy XYZ, where X and Y are transitional metals and Z is the main group element, has only one magnetic sublattice. Half-Heusler materials are related to classic semiconductors like Si and GaAs, and they crystallize into the non-centrosymmetric cubic MgAgAs-$C1_b$ structure (space group F-43m, No.216) with a 1:1:1 stoichiometry, which is arranged differently from CaF_2 and may originate from the tetrahedraL zinc blend (ZB)-type structure [64].

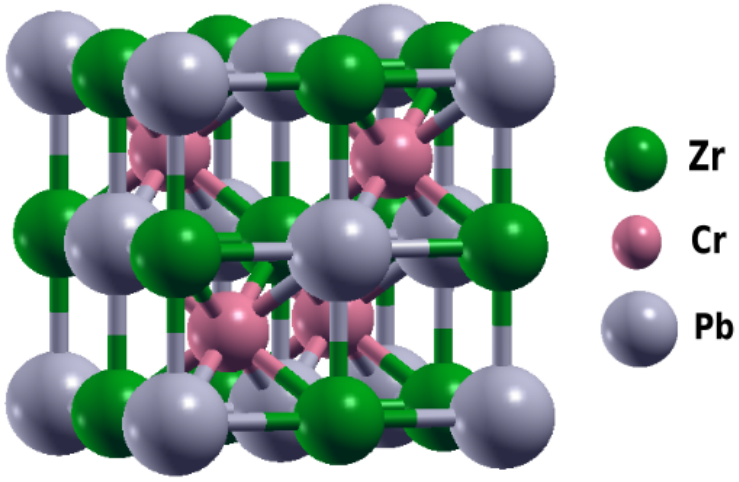

Figure 3.1: Crystallographic structure of half-Heusler alloy ZrCrPb.

The three inter-penetrating fcc lattices Wyckoff positions are 4a(0, 0, 0), 4b(1/2, 1/2, 1/2) and 4c(1/4, 1/4, 1/4) while 4d(3/4, 3/4, 3/4) site is unoccupied. In essence, these Wyckoff locations 4a, 4b and 4c can be occupied by X, Y and Z atoms, respectively. For an illustration, the crystal structure of ZrCrPb alloy for possible atomic arrangements is shown in Figure 3.1. The lattice constant is calculated using Murnaghan's equation of state [65]. The most stable structure of ZrCrPb is confirmed by optimizing the total energy as a function of volume for the states with the lattice parameter 6.5643 Å as illustrated in Figure 3.2. The results after SCF calculation are shown in Table 3.1.

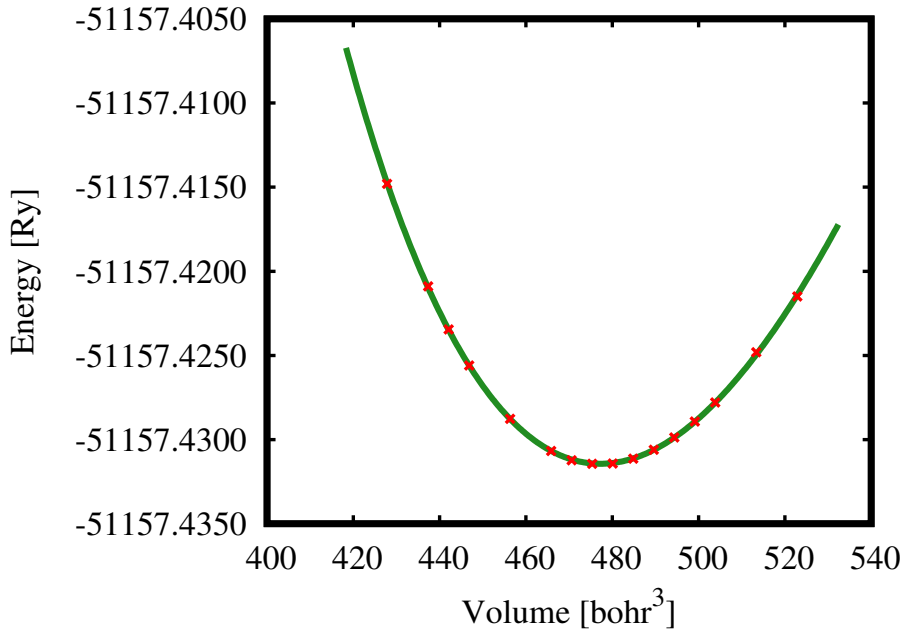

Figure 3.2: Calculated total energy of ZrCrPb alloy as a function of unit cell volume

Table 3.1: Calculated total energy (Ry) and fermi energy (eV).

Compound	Exchange correlation potential	Total energy (Ry)	Fermi energy (eV)
ZrCrPb	PBE-GGA	-51157.43143	0.5196

3.3 Electronic properties

The electronic structures contain an essential part to identify the half-metallic properties associated with half-Heusler materials. Its crucial to compute the band structures and density of states (DOS) of a crystalline solid in order to understand its electronic properties, which usually always explain the system's transport and optical properties. With the PBE approximation, the estimated electronic band structures, total density of states (TDOS) and total contribution of ZrCrPb alloy are displaced in Figure 3.3 within energy range -4 to 4 eV. The left panel exhibits the spin-up (majority) state, and the right panel demonstrates the bands for the spin-down (minority) state. The different colors in Figure 3.3 show different physical meanings. They show the contributions of s, p and d orbitals of Zr, Cr and Pb atoms to electronic band structures. Dashed lines are indicating fermi level (zero

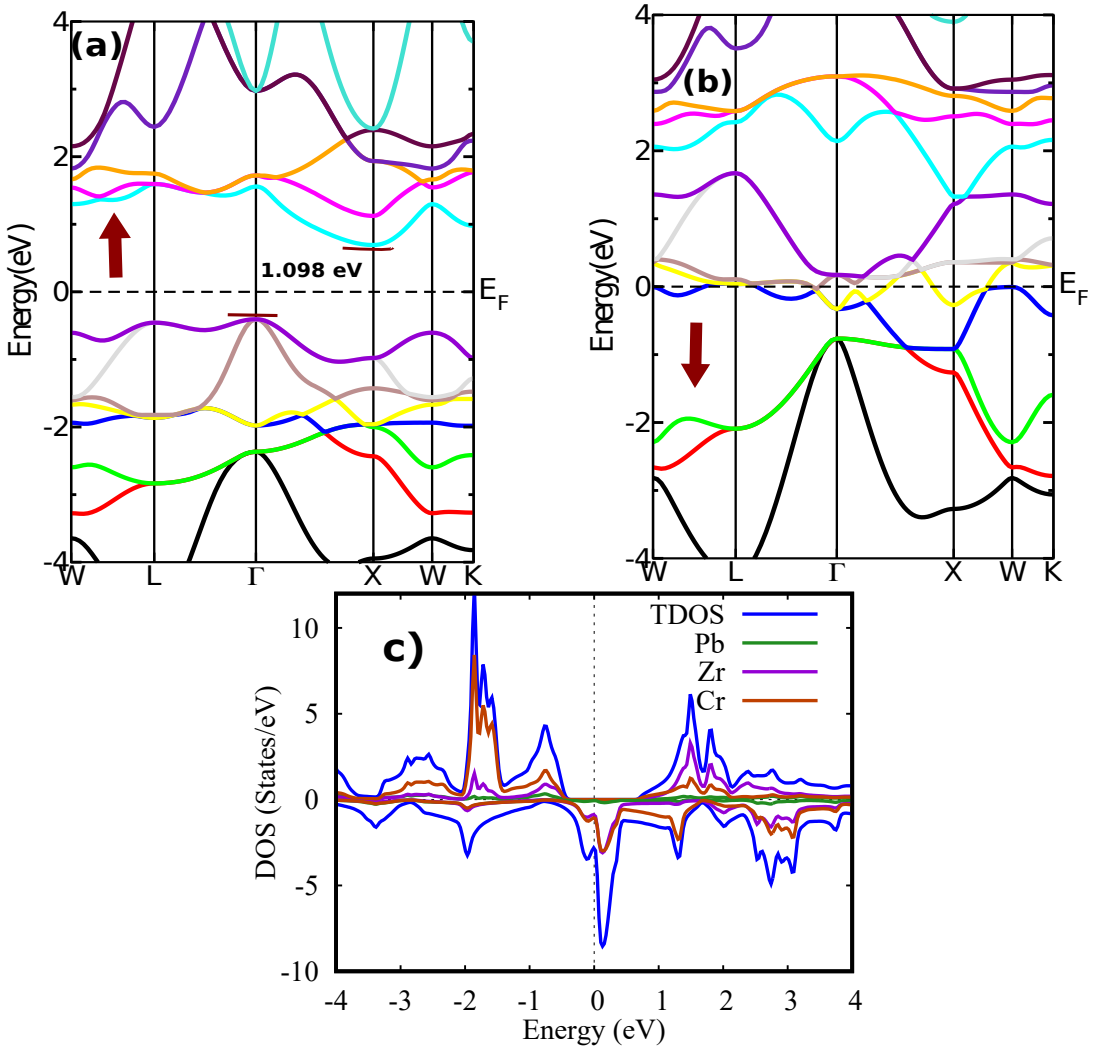

Figure 3.3: Electronic band structures of ZrCrPb a) up spin b) down spin and c) Total Density of States (TDOS).

energy) and all the properties are calculated in the first Brillouin zone through the high symmetry paths. For up spin, conduction band minimum is on the X point, while the valnace band maximum is on the Γ point providing an indirect band gap of 1.098 eV as shown in Figure 3.3(a). But there is no band gap for down spin (Figure 3.3(b)), which illustrates the compound half-metallic nature. The number of states filled by distinct energy levels for each period of energy is referred to as the density of states (DOS). Figure 3.3(c) represents the total density of states of ZrCrPb alloy. In the system, we see that the total contribution of Pb in the valance band and conduction band is negligible. ZrCrPb has half-metallicity due to Zr and Cr down spin. The partial density of states (PDOS) of a system represents how holes and electrons arrange themselves within a solid and other optical characteris-

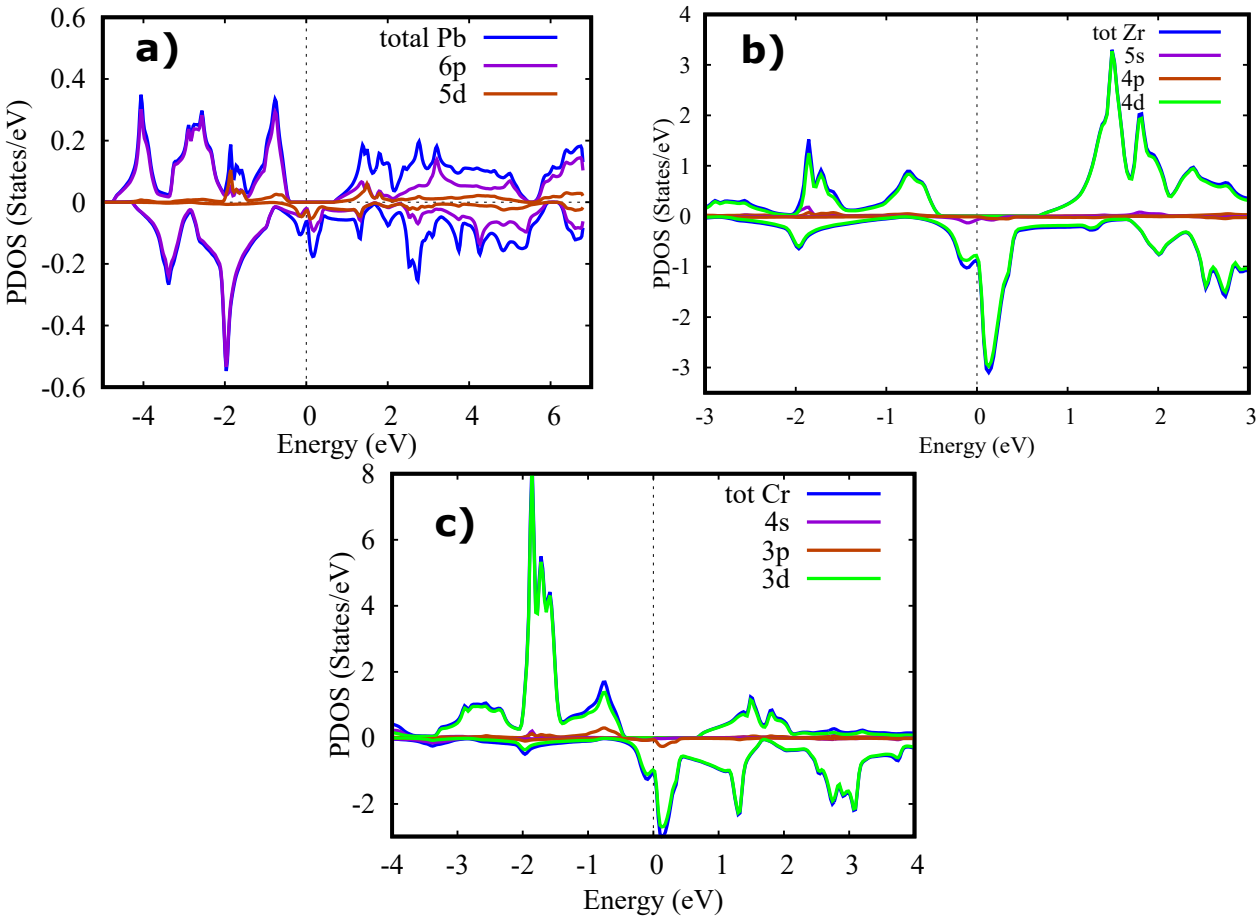

Figure 3.4: Partial density of states (PDOS) of ZrCrPb a) Pb b) Zr and c) Cr atoms.

tics. The PDOS of ZrCrPb alloy is the representation of the hybridization of Zr-4d, Cr-3d, and Pb-6p atoms where Pb-6p is dominated in valance band and Zr-4d and Cr-3d dominated in conduction band. In down spin, metallicity appears due to the hybridization of Zr-4d and Cr-3d atoms in the Fermi level. In comparison to Zr and Cr atoms, the contribution of the Pb atom at Fermi level is minor. Zr and Cr d orbitals contribute the majority of states near E_f for down spin, which is consistent to other transition metal-based half-Heusler computations. The up spin state in the alloy has a semiconducting property with an energy gap around Fermi level, but the down spin state cross the Fermi level and exhibits metallic behaviour, indicating that the examined material is half metallic with 100% spin polarization. Figure 3.4 represents the partial density of states (PDOS) of ZrCrPb.

3.4 Magnetic properties

The unsymmetrical character of up and down spin charge density distribution and density of states causes the magnetic properties of ZrCrPb alloy. As half-Heusler materials have single magnetic sublattice on its octahedral sites, mainly Zr atom occupies the octahedralsites in stable structure of ZrCrPb alloy. Magnetic moments in pure metals fluctuate according to Hund's rule, but when Heusler transition metals form alloys, the d orbital electron availability changes due to the different electro-negativity [30] of the transition metals in the periodic table.

Table 3.2: Magnetic moments in terms of Bohr magneton (μ_B) for Zr, Cr and Pb atoms respectively and total magnetic moment of ZrCrPb alloy.

Compound	M_{Zr}/μ_B	M_{Cr}/μ_B	M_{Pb}/μ_B	M_{int}/μ_B	M_{tot}/μ_B	Magnet type
ZrCrPb	0.28447	3.24772	-0.01407	0.48233	4.00045	Ferromagnet

Table 3.2 shows the total and interestitial magnetic moments of ZrCrPb alloy in unit of Bohr magneton (μ_B), as well as individual moments of Zr, Cr, and Pb respectively. From total magnetic moments it can be seen that the alloy is ferromagnetic in nature. This material can be used to make transformers, generators, electric motors, hard drives, hard disks, magnetic storage, magnetic tape recording, and other electromagnetic devices.

3.5 Optical properties

In order to understand the optical properties of half-Heusler alloy, we have studied the dielectric tensor (ϵ), absorption coefficient (A), conductivity, reflectivity (R), and refractive index (η) of ZrCrPb alloy.

3.5.1 Dielectric function

There are two parts of dielectric function, which are imaginary dielectric function and real dielectric function. The mathematical formula for dielectric function as

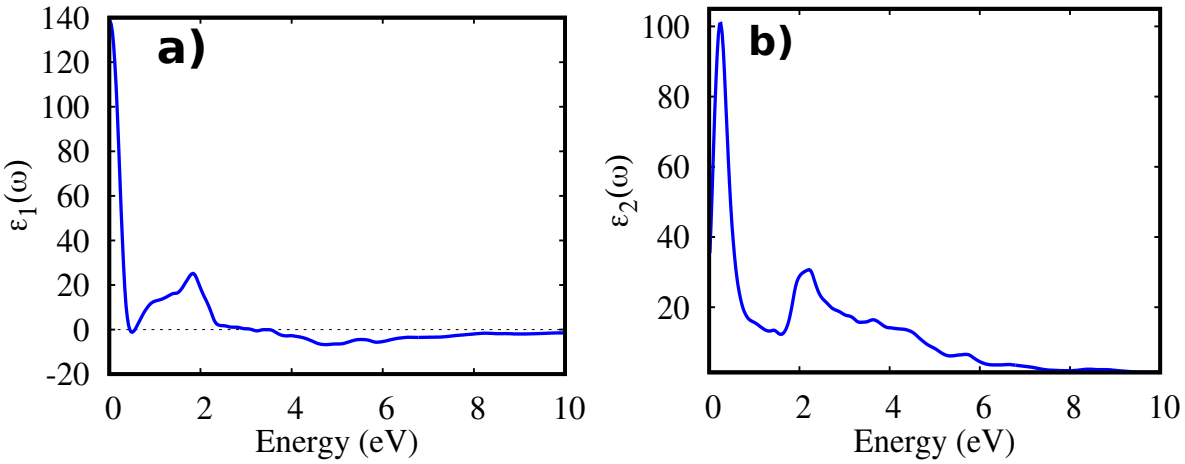

Figure 3.5: Dielectric function a) real b) imaginary

given by Ehrenreich and Cohen's is, [66]

$$\epsilon(\omega) = \epsilon_1(\omega) + i\epsilon_2(\omega) \tag{3.1}$$

where, ϵ_1 and ϵ_2 are the real and imaginary part of the dielectric function. Real dielectric function ($\epsilon_1(\omega)$) represents the degree of polarization of a material when it placed into an electric field and imaginary dielectric function ($\epsilon_2(\omega)$) represents the energy dissipation aptitude of a dielectric material. The dielectric function is physically analogous to the absolute permittivity in terms of its relationship to the space materials. Figure 3.5(a) and 3.5(b) represent the real and imaginary dielectric functions of ZrCrPb alloy with respect to the photon energy renges from 0 to 12 eV. Figure 3.5(b) represents the imaginary part of dielectric function having maximum losses at smaller energy range which predicts the half-metallic character of the alloy.

3.5.2 Absorption coefficient

Absorption of photons occur during the transition of an electron from an unoccupied to an occupied state. Figure 3.6(a) represents the absorption coefficient of ZrCrPb alloy with PBE approximation method. It can be observed in Figure 3.6(a) that absorptivity increases progressively in the infrared and visible region, reaches a maximum at 5 eV (ultra-violet region), and decreases with increasing energy values. The absorption peak demonstrates that this material can absorb photons in both the ultra-violet and visible ranges.

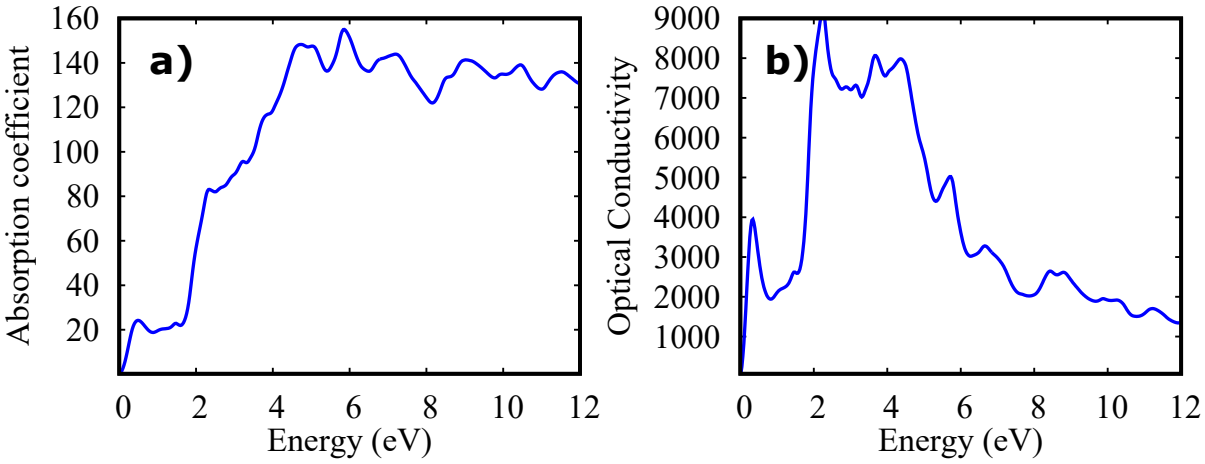

Figure 3.6: a) Absorption coefficient b) Optical conductivity

3.5.3 Optical conductivity

The energy gap between the valance and conduction bands in semiconductors is lower than in insulators. As a result, semiconductors are semi-good conductors with a valance band that is completely vacant. The optical conductivity of computed alloy is shown in Figure 3.6(b). It demonstrates that conductivity is highest in the visible range for the alloy.

3.5.4 Reflectivity

Optical reflectivity is another parameter which plays a vital role in shifting electron from valance band to the conduction band. The amount of energy absorbed, reflected, and transmitted by a material is equal to the incident photon energy. Estimating the absorbance and transmittance of the substance on which light is incident it is possible to compute the total amount of ray incident on the surface of a semiconductor.

$$A + R + T = 1 \tag{3.2}$$

where, A, R, and T represents the absorbance, reflectance, and transmittance of a material respectively. The optical reflectivity of estimated half-Heusler alloy is shown in Figure 3.7(a).

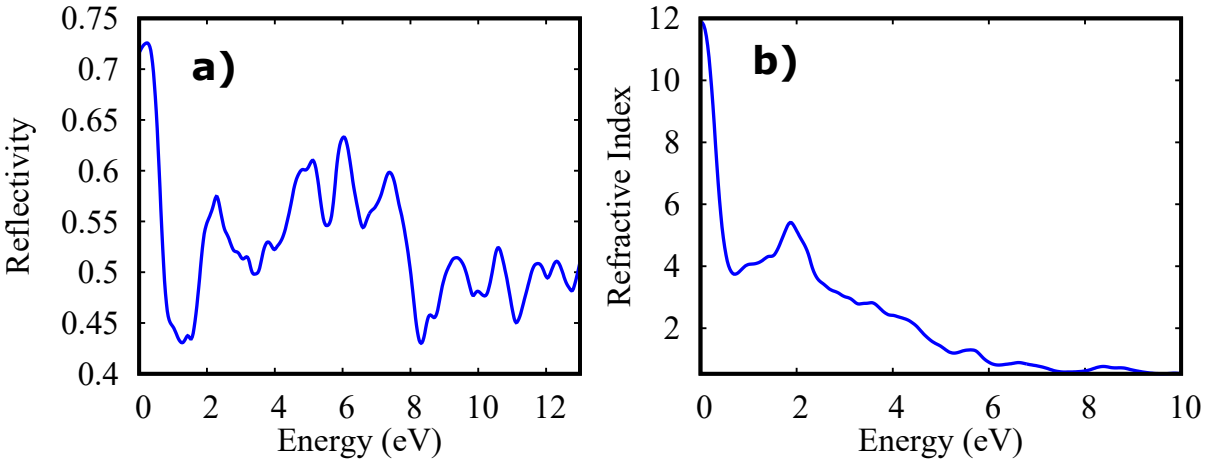

Figure 3.7: a) Reflectivity b) Refractive index

3.5.5 Refractive index

Refraction index indicates that the quantity of light bending is highest in the infrared range in the visible zone. The presence of these peaks in the infrared suggest that the refractive index of half-Heusler alloy is non-linear in nature. The refractive index of the computed ZrCrPb alloy is shown in Figure 3.7(b). In conclusion, due of the non linear absorbing capability and refractive index, the computed half-Heusler alloy can be used in electro-mechanical applications that can absorb photons in both the ultra-violet and visible regions.

Chapter 4

Conclusions

We investigated the electronic, magnetic and optical properties of half-Heusler ZrCrPb alloy using WIEN2k in the context of density functional theory and the PBE approximation approach. The electronic and magnetic characteristics of the alloy with the lowest energy were calculated. For up spin, the system estimates an indirect band gap, providing a non-metallic character, whereas the system produces a metallic band for down spin. As a result, electrical properties of the system are half-metallic in nature. The magnetic moment of system is around 4 μ_B, indicating the ferromagnetic contribution of the alloy. The optical absorptivity, conductivity, reflectivity, refractive index and dielectric functions of the system were also investigated. From imaginary dielectric function, we got the half-metallic character of the alloy.

List of Abbreviations

BZ	:	Brillouin Zone
DFT	:	Density Functional Theory
DOS	:	Density of States
XC	:	Exchange Correlation
FP-LAPW	:	Full-Potential Linear Augmented Plane Wave
GGA	:	Generalized Gradient Approximation
HK	:	Hohenberg-Kohn
HM	:	Half Metallic
KS	:	Kohn-Sham
PBE	:	Perdew-Burke-Ernzerhof
ZnS	:	Zinc Blende

Bibliography

[1] Ramit Kumar Mondal, Sonachand Adhikari, Vijay Chatterjee, and Suchandan Pal. Recent advances and challenges in algan-based ultra-violet light emitting diode technologies. *Materials Research Bulletin*, 140:111258, 2021.

[2] Ha Hwang, Deok Hyeon Yoon, Im Hyuk Shin, In Seon Yoon, Jin Ho Kwack, OukJae Lee, Young Wook Park, and Byeong-Kwon Ju. Spin-polarized carrier injection through hybrid ferromagnetic electrode for enhanced optical efficiency of organic light-emitting diodes. *Organic Electronics*, 84:105755, 2020.

[3] J Rudolph, S Döhrmann, D Hägele, M Oestreich, and W Stolz. Room-temperature threshold reduction in vertical-cavity surface-emitting lasers by injection of spin-polarized electrons. *Applied Physics Letters*, 87(24):241117, 2005.

[4] Neetu Gyanchandani, Santosh Pawar, Prashant Maheshwary, and Kailash Nemade. Preparation of spintronically active ferromagnetic contacts based on fe, co and ni graphene nanosheets for spin-field effect transistor. *Materials Science and Engineering: B*, 261:114772, 2020.

[5] Gul Faroz Ahmad Malik, Mubashir Ahmad Kharadi, and Farooq Ahmad Khanday. Electrically reconfigurable logic design using multi-gate spin field effect transistors. *Microelectron. J.*, 90:278–284, 2019.

[6] Yuuki Sato, Shin-ichiro Gozu, Tomohiro Kita, and Syoji Yamada. Study for realization of spin-polarized field effect transistor in in0. 75ga0. 25as/in0. 75al0. 25as heterostructure. *Physica E: Low-dimensional Systems and Nanostructures*, 12(1-4):399–402, 2002.

[7] Ming-Cheng Kao, Hone-Zern Chen, Kai-Huang Chen, Jen-Bin Shi, Jun-Hong Weng, and Kuan-Po Chen. Resistive switching behavior and optical properties of transparent pr-doped zno based resistive random access memory. *Thin Solid Films*, 697:137816, 2020.

[8] Yumei Zhang, Wen Zhang, Mengyao Ning, Lingli Chen, and Haibo Li. Tuning the magnetism of l10-mnga films by pt doping. *Applied Surface Science*, 542:148585, 2021.

[9] Heiddy P Quiroz, Jorge A Calderón, and A Dussan. Magnetic switching control in co/tio2 bilayer and tio2: Co thin films for magnetic-resistive random access memories (m-rram). *Journal of Alloys and Compounds*, 840:155674, 2020.

[10] Chi Liu, Tao Shen, Hai-Bin Wu, Yue Feng, and Jiao-Jiao Chen. Applications of magneto-strictive, magneto-optical, magnetic fluid materials in optical fiber current sensors and optical fiber magnetic field sensors: A review. *Optical Fiber Technology*, 65:102634, 2021.

[11] Nouha Alcheikh, S Ben Mbarek, HM Ouakad, and MI Younis. A highly sensitive and wide-range resonant magnetic micro-sensor based on a buckled micro-beam. *Sensors and Actuators A: Physical*, 328:112768, 2021.

[12] Atsufumi Hirohata, Keisuke Yamada, Yoshinobu Nakatani, Ioan-Lucian Prejbeanu, Bernard Diény, Philipp Pirro, and Burkard Hillebrands. Review on spintronics: Principles and device applications. *Journal of Magnetism and Magnetic Materials*, 509:166711, 2020.

[13] Amal El-Ghazaly, Jon Gorchon, Richard B Wilson, Akshay Pattabi, and Jeffrey Bokor. Progress towards ultrafast spintronics applications. *Journal of Magnetism and Magnetic Materials*, 502:166478, 2020.

[14] R Umamaheswari, M Yogeswari, and G Kalpana. Ab-initio investigation of half-metallic ferromagnetism in half-heusler compounds xyz (x= li, na, k and rb; y= mg, ca, sr and ba; z= b, al and ga). *Journal of magnetism and magnetic materials*, 350:167–173, 2014.

[15] Fr Heusler, W Starck, and E Haupt. Magnetisch-chemische studien. *Verh. Dtsch. Phys. Ges*, 5:219–232, 1903.

[16] F Heusler. Magnetic-chemical studies verh. *Dtsch. Phys. Ges*, 5:219, 1903.

[17] Jonah Nagura, Timothy M Ashani, Paul O Adebambo, F Ayedun, and Gboyega A Adebayo. Thermoelectric and mechanical properties of xhfsn (x= ni, pd and pt) semiconducting half-heusler alloys: a first-principles study. *Computational Condensed Matter*, 26:e00539, 2021.

[18] Yuhit Gupta, MM Sinha, and SS Verma. Investigations of mechanical and thermoelectric properties of 'alnip'novel half-heusler alloy. *Materials Chemistry and Physics*, 265:124518, 2021.

[19] Evren G Özdemir and Ziya Merdan. Half-metal calculations of cozrge half-heusler compound by using generalized gradient approximation (gga) and modified becke-johnson (mbj) methods. *Materials Research Express*, 6(11):116124, 2019.

[20] Kulwinder Kaur and Jaswinder Kaur. Exploration of thermoelectricity in scrhte and zrptpb half heusler compounds: A first principle study. *Journal of Alloys and Compounds*, 715:297–303, 2017.

[21] P Sivaprakash, S Esakki Muthu, Anupam K Singh, KK Dubey, M Kannan, S Muthukumaran, Shampa Guha, Manoranjan Kar, Sanjay Singh, and S Arumugam. Effect of chemical and external hydrostatic pressure on magnetic and magnetocaloric properties of pt doped ni2mnga shape memory heusler alloys. *Journal of Magnetism and Magnetic Materials*, 514:167136, 2020.

[22] Evren G Özdemir and Ziya Merdan. First-principles predictions on structural, electronic, magnetic and elastic properties of mn2iral heusler alloy. *Materials Research Express*, 6(3):036101, 2018.

[23] RM Shabara and BO Alsobhi. Calculations of the structural, elastic, and magnetic properties of the novel full heusler alloys ru2xy with x= nb, mn and y= te, sb. *JETP Letters*, 113(5):322–330, 2021.

[24] Y Venkateswara, Deepika Rani, KG Suresh, and Aftab Alam. Half-metallic ferromagnetism and ru-induced localization in quaternary heusler alloy corumnsi. *Journal of Magnetism and Magnetic Materials*, 502:166536, 2020.

[25] K Benkaddour, Abbes Chahed, Amina Amar, Habib Rozale, Abdelaziz Lakdja, Omar Benhelal, and Adlane Sayede. First-principles study of structural, elastic, thermodynamic, electronic and magnetic properties for the quaternary heusler

alloys corufez (z= si, ge, sn). *Journal of Alloys and Compounds*, 687:211–220, 2016.

[26] S Bahramian and F Ahmadian. Half-metallicity and magnetism of quaternary heusler compounds corutiz (z= si, ge, and sn). *Journal of Magnetism and Magnetic Materials*, 424:122–129, 2017.

[27] Evren G Özdemir and Ziya Merdan. First-principles calculations to investigate half-metallic band gap and elastic stability of co (mo, tc) mnsb compounds. *Physica E: Low-dimensional Systems and Nanostructures*, 133:114790, 2021.

[28] Nazir Ahmad Teli and M Mohamed Sheik Sirajuddeen. A dft study of the structural, elastic, electronic and magnetic properties of new quaternary compounds tihfosx (al, ga, in). *Physics Letters A*, 384(32):126793, 2020.

[29] RA De Groot, FM Mueller, PG Van Engen, and KHJ Buschow. New class of materials: half-metallic ferromagnets. *Physical Review Letters*, 50(25):2024, 1983.

[30] M Atif Sattar, Muhammad Rashid, M Raza Hashmi, SA Ahmad, Muhammad Imran, and Fayyaz Hussain. Theoretical investigations of half-metallic ferromagnetism in new half–heusler ycrsb and ymnsb alloys using first-principle calculations. *Chinese Physics B*, 25(10):107402, 2016.

[31] Manoj K Yadav and Biplab Sanyal. First principles study of thermoelectric properties of li-based half-heusler alloys. *Journal of Alloys and Compounds*, 622:388–393, 2015.

[32] David J Griffiths and Darrell F Schroeter. *Introduction to quantum mechanics*. Cambridge university press, 2018.

[33] GEORGE NIKOULIS and JOSEPH KIOSEOGLOU. Computational analysis of charge distribution of pd nanoparticles on mg and mgo substrates.

[34] E Schrödinger. Schrödinger 1926e. *Annalen der Physik*, 81:109, 1926.

[35] F Schwabl. Quantum mechanics (qm i). ; quantenmechanik (qm i). eine einfuehrung. 2007.

[36] DJ Griffiths. Introduction to quantum mechanics 2nd ed.-solutions. 2005.

[37] Max Born. Quantenmechanik der stoßvorgänge. *Zeitschrift für physik*, 38(11):803–827, 1926.

[38] David C Young. Density functional theory. *Computational Chemistry*, pages 42–48, 2001.

[39] Wolfgang Pauli. The connection between spin and statistics. *Physical Review*, 58(8):716, 1940.

[40] Arthur Jabs. Connecting spin and statistics in quantum mechanics. *Foundations of Physics*, 40(7):776–792, 2010.

[41] Attila Szabo and Neil S Ostlund. *Modern quantum chemistry: introduction to advanced electronic structure theory*. Courier Corporation, 2012.

[42] Wolfgang Pauli. On the connexion between the completion of electron groups in an atom with the complex structure of spectra. *Zeitschrift für Physik*, 31:765, 1925.

[43] Nouredine Zettili. Quantum mechanics: concepts and applications, 2003.

[44] Klaus Capelle. A bird's-eye view of density-functional theory. *Brazilian journal of physics*, 36:1318–1343, 2006.

[45] Niklas Zwettler. Density functional theory.

[46] Paul Adrien Maurice Dirac. A new notation for quantum mechanics. In *Mathematical Proceedings of the Cambridge Philosophical Society*, volume 35, pages 416–418. Cambridge University Press, 1939.

[47] Christian B Lang and Norbert Pucker. *Mathematische methoden in der physik*, volume 2. Springer, 2005.

[48] Walter Kohn. Nobel lecture: Electronic structure of matter—wave functions and density functionals. *Reviews of Modern Physics*, 71(5):1253, 1999.

[49] Per-Olov Löwdin. Scaling problem, virial theorem, and connected relations in quantum mechanics. *Journal of Molecular Spectroscopy*, 3(1-6):46–66, 1959.

[50] Pierre Hohenberg and Walter Kohn. Inhomogeneous electron gas. *Physical review*, 136(3B):B864, 1964.

[51] Reiner M Dreizler and Eberhard KU Gross. *Density functional theory: an approach to the quantum many-body problem*. Springer Science & Business Media, 2012.

[52] Klaus Capelle, Carsten A Ullrich, and Giovanni Vignale. Degenerate ground states and nonunique potentials: Breakdown and restoration of density functionals. *Physical Review A*, 76(1):012508, 2007.

[53] Lu Jeu Sham and Walter Kohn. One-particle properties of an inhomogeneous interacting electron gas. *Physical Review*, 145(2):561, 1966.

[54] Robert G Parr. Density functional theory of atoms and molecules. In *Horizons of quantum chemistry*, pages 5–15. Springer, 1980.

[55] Hongmei Wang and Yunbo Zhang. Density-functional theory for the spin-1 bosons in a one-dimensional harmonic trap. *Physical Review A*, 88(2):023626, 2013.

[56] Yayun Hu, G Murthy, Sumathi Rao, and JK Jain. Kohn-sham density functional theory of abelian anyons. *Physical Review B*, 103(3):035124, 2021.

[57] Jianmin Tao, John P Perdew, Viktor N Staroverov, and Gustavo E Scuseria. Climbing the density functional ladder: Nonempirical meta–generalized gradient approximation designed for molecules and solids. *Physical Review Letters*, 91(14):146401, 2003.

[58] Peter Blaha, Karlheinz Schwarz, P Sorantin, and SB Trickey. Full-potential, linearized augmented plane wave programs for crystalline systems. *Computer physics communications*, 59(2):399–415, 1990.

[59] Peter Blaha, Karlheinz Schwarz, Georg KH Madsen, Dieter Kvasnicka, Joachim Luitz, et al. wien2k. *An augmented plane wave+ local orbitals program for calculating crystal properties*, 60, 2001.

[60] P Kepple and Hans R Griem. Improved stark profile calculations for the hydrogen lines h α, h β, h γ, and h δ. *Physical Review*, 173(1):317, 1968.

[61] Weine Olovsson, I Tanaka, Peter Puschnig, and C Ambrosch-Draxl. Near-edge structures from first principles all-electron bethe–salpeter equation calculations. *Journal of Physics: Condensed Matter*, 21(10):104205, 2009.

[62] John P Perdew, Kieron Burke, and Matthias Ernzerhof. D. of physics and nol 70118 j. quantum theory group tulane university. *Phys. Rev. Lett*, 77:3865–3868, 1996.

[63] O Jepson and OK Anderson. The electronic structure of hcp ytterbium. *Solid state communications*, 88(11-12):871–875, 1993.

[64] Tanja Graf, Claudia Felser, and Stuart SP Parkin. Simple rules for the understanding of heusler compounds. *Progress in solid state chemistry*, 39(1):1–50, 2011.

[65] Francis Dominic Murnaghan. Finite deformations of an elastic solid. *American Journal of Mathematics*, 59(2):235–260, 1937.

[66] Nasir Mehmood and Rashid Ahmad. Structural, electronic, magnetic, and optical properties of half-heusler alloys rumnz (z= p, as): a first-principle study. *Journal of Superconductivity and Novel Magnetism*, 31(1):233–239, 2018.